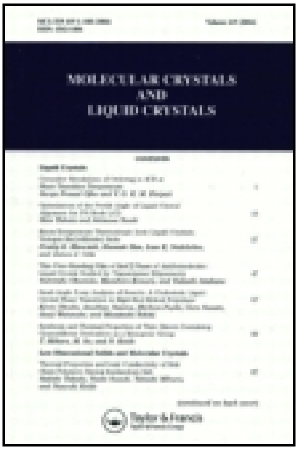

Molecular Crystals and Liquid Crystals Science and Technology. Section A. Molecular Crystals and Liquid Crystals

Publication details, including instructions for authors and subscription information:
http://www.tandfonline.com/loi/gmcl19

Nanoscale Chemistry and Processing of Multifunctional Composites for Nanophotonics and Biophotonics

Christopher S. Friend [a], Manjari Lal [a], Abani Biswas [a], Glauco S. Maciel [a], Laurent Levy [a], Guang S. He [a], Kyoung-Soo Kim [a] & Paras N. Prasad [a]

[a] Institute for Lasers, Photonics, and Biophotonics, State University of New York at Buffalo, Buffalo, New York, 14260-3000

Version of record first published: 24 Sep 2006

To cite this article: Christopher S. Friend, Manjari Lal, Abani Biswas, Glauco S. Maciel, Laurent Levy, Guang S. He, Kyoung-Soo Kim & Paras N. Prasad (2000): Nanoscale Chemistry and Processing of Multifunctional Composites for Nanophotonics and Biophotonics, Molecular Crystals and Liquid Crystals Science and Technology. Section A. Molecular Crystals and Liquid Crystals, 353:1, 257-270

To link to this article: http://dx.doi.org/10.1080/10587250008025665

Mol. Cryst. and Liq. Cryst., 2000, Vol. 353, pp. 257-270
Reprints available directly from the publisher
Photocopying permitted by license only

Nanoscale Chemistry and Processing of Multifunctional Composites for Nanophotonics and Biophotonics

CHRISTOPHER S. FRIEND, MANJARI LAL, ABANI BISWAS, GLAUCO S. MACIEL, LAURENT LEVY, GUANG S. HE, KYOUNG-SOO KIM and PARAS N. PRASAD

Institute for Lasers, Photonics, and Biophotonics, State University of New York at Buffalo, Buffalo, New York 14260–3000

Multifunctional nanostructured materials and composites are of considerable interest for photonics, optoelectronics and biophotonics. This paper will focus on three topics. In the first part of the paper, we will focus on silica encapsulated multifunctional nanoparticles. These particles show enhanced optical properties as well as photo, chemical and thermal stability. In the second part of the paper, we investigate the Er^{3+} sol-gel multicomponent silica glass prepared with nanostructure control for 1.55 μm amplification. These glasses demonstrate the longest reported lifetime in sol-gel glasses to date, which we attribute to the reduction of the hydroxyl content in the glass. The third part of the paper discusses our work on photonic crystals.

Keywords: nanoparticle; rare-earth; sol-gel; photonic crystal

INTRODUCTION

As we start a new millenium, our daily life is becoming more dependent on advanced technology. The implementation of any new technology is crucially dependent on the availability of suitable materials, because without it, a technology is just a concept. The realization of this advanced

technology rests on the development of multifunctional materials that simultaneously satisfy many requirements[1,2]. Nanoparticles, which exhibit different properties compared to the bulk properties, are a new generation of materials that hold considerable promise for numerous applications in the fields of electronics, photonics and biophotonics. Nanoscale modification of molecular design and morphology provides a powerful approach to control electronic and optical properties of a material as well as its processability. These properties include quantum size effect on photochemistry[3], nonlinear optical properties of semiconductors[4,5] and metallic clusters[6,7]. This review describes the synthesis and characterization of three new materials: silica nanobubbles, Er^{3+} doped sol gel multicomponent silica glass and photonic crystals.

Inorganic probes made from metal and semiconductor nanoparticles have shown great promise in applications such as sensors, biosensors, and for cell imaging[8-10]. Incorporation of organic chromophores within bulk inorganic matrices for solid state lasers, nonlinear optical materials and optical data storage has been pursued with great interest[11]. However, the incorporation of fluorescent chromophores within inorganic nanoparticles is a newly emerging field[12]. In this area, two-photon chromophores will have many advantages over single-photon chromophores for 3-dimensional microfabrication[13], optical data storage[14,15] and cell imaging[16]. The use of two-photon excitation reduces photobleaching and photodamage of the chromophore, but more importantly it allows for infrared excitation. This longer wavelength has been shown[17] to have little or no effect on the viability of living cells as compared to visible wavelengths during the extended imaging of living embryos in culture tubes. Thus, prolonged *in* *vivo* imaging can be done. Unfortunately, most two-photon chromophores are highly hydrophobic and their emission is quenched by water. To overcome this drawback, encapsulation of these dyes within silica renders them water dispersible. It also provides an inert barrier to the external environment, which leads to an enhancement of the optical properties of the chromophore. This occurs due to the minimization of the solvent effects responsible for nonradiative decay mechanisms.

There is great interest in optically transparent functional materials that operate at the telecommunications wavelength of 1.55 μm and 1.30 μm. These materials have applications in optical fiber telecommunications, medical diagnostics and applications, data storage, displays and IR detection cards. Sol gel processed materials with nanostructure control show great promise in these areas since they can provide the necessary stability and processability for these applications.

In the field of microporous materials, a special class of dielectric structures exists that exhibit periodicity in three dimensions. These are called photonic crystals. When the dielectric contrast within the structure is high, a photonic bandgap occurs. These photonic bandgap materials can manipulate light in the same manner that a semiconductor manipulates electrons. Applications of these materials include low threshold lasers, switches and all-optical transistors for use in optical telecommunications, optical data transfer and all optical computing.

I. Silica Encapsulated Multifunctional Nanoparticles.

In our work, the synthesis of a dye doped composite silica nanoparticle is achieved by carrying out the reaction within a reverse micellar cavity. This approach of nanocompartmentalization[18] has already been used extensively in the area of material science for preparing various metallic nanoparticles[19], semiconductor nanoclusters[20] and polymeric nanoparticles[21]. The interest stems mainly from the diversity in the organized structures that are formed under different compositional and operational conditions using the reverse micelle approach. Reduction of the particle size to a nanometer level has potential benefits, which manifests by remarkably changing the physicochemical properties, the most noticeable being the quantum size effect observed in semiconductor nanoparticles[22]. The other effects are enhanced electric and magnetic properties of metallic particles and nanoclusters[23]. The highlighting feature of reverse micelle synthesis is size tunability which arises as a result of confining a reaction to nanometer sized aqueous droplets characterized by a size parameter, W_O (W_O=[H_2O]/[Surfactant]). The exchange rate and dynamics of these droplets influence the particle growth and nucleation, thereby governing the particle size[24]. The changes in particle size can also be obtained by modifying the absolute and relative reactant concentrations, which are expected to be of significance in the formation of complex structures and composites[25,26].

Using reverse micelle mediated synthesis, we have prepared ZnS/dye/SiO_2 heterostructured nanoparticles through multistep reaction. Specifically, by subsequent reaction and chemical processing within the cavity, we made inorganic-organic particles of zinc sulfide in the core surrounded by a two-photon dye ASPI-SH which is attached to the semiconductor through the thiol group. Zinc sulfide was chosen as the semiconductor since its band gap is well separated from that of the chromophore. In other words, there is no spectral overlap between zinc sulfide and the dye. During the reaction, the nucleus of zinc sulfide grows to a desired/required size (W_O), then the surface of these nanocrystallites is passivated or capped through covalent addition of the dye (ASPI-SH) thiol which serves not only as the source of sulfide ions but also as a growth moderator[27]. This property stems from the ability of thiolate ions to bind to the metal ions on the semiconductor surface, thereby effectively inhibiting the growth of the semiconductor nanoparticles. This process was followed by the introduction of a sol-gel silica precursor, tetraethoxyorthosilicate (TEOS), which undergoes hydrolysis in the aqueous core forming a silica shell around the dye capped zinc sulfide particles. The advantage of using TEOS as the silica precursor is its relatively slow and controllable rate of reaction. Furthermore, the reverse micelle technique is versatile and can be used for the synthesis of other kinds of hybrid materials.

There are several advantages of using a silica shell as a stabilizer. Silica is chemically inert and, therefore, does not affect the redox reaction at the core surface. The shell is optically transparent; furthermore, the shell prevents coagulation during chemical reactions and concentrated dispersions of nanosized semiconductors can be made. Also, the silica shell acts as a barrier, limiting the effect of the outside environment on the core particles. This is particularly important for two-photon dyes, which are sensitive to certain solvents, especially water, which quench the emission due to certain nonradiative decay processes.

The fluorescence spectra of the free dye and the dye encapsulated within silica nanobubbles are shown in figures 1a and 1b respectively. The fluorescence yield of the free dye is lower relative to the encapsulated dye. This behavior may be due to certain non-radiative decay mechanisms which

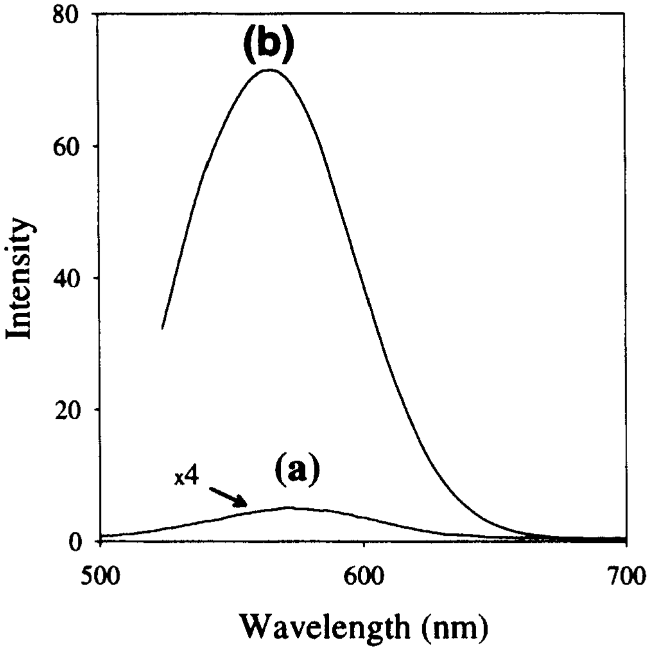

Figure 1 Fluorescence spectra of (a) the free dye magnified 4x and (b) the dye encapsulated within silica nanobubbles. Both are dissolved in water.

may arise as a result of Twisted Intramolecular Charge Geometry acquired in the dye as a result of electron transfer from the donor group to the acceptor group. The extent of the charge transfer process is strongly dependent on the polarity of the solvent. The protective barrier provided by silica blocks the external solvent influence to enhance the fluorescence quantum yield. Hence the non-radiative decay processes which are solvent dependent and are responsible for low fluorescence yield are prevented.

We observed that the lifetime of the encapsulated dye particles (300ps) was longer than the lifetime for the free dye molecule (80 ps), which indicates that the dye particles are shielded from the outside environment.

We also demonstrated that silica encapsulation of the chromophore leads to enhanced photo, chemical, and thermal stability of the chromophore. We have recently used these nanoparticles for biological imaging.

II. Er^{3+} Sol-Gel Multicoponent Silica Glass.

Silica glass is a highly attractive matrix for optical applications due to its favorable thermal and mechanical properties[29]. Rare earth doped silica glasses are potential materials for solid state fiber lasers[30], amplifiers[31] and upconversion lasers[32]. There have been several attempts to make Er-doped glasses by the sol-gel method for optical applications. However, the success was severely restricted by the fact that the rare earth ions have a tendency to have a nonuniform distribution and form clusters in the bulk, which reduce the fluorescence efficiency and lifetime[33]. The presence of a large concentration of hydroxyl groups in the sol-gel glasses also degrades the emission properties[34]. In order to prepare device quality silica glasses doped with rare earth ions, the hydroxyl quenching and ion clustering must be eliminated. A process has been developed to make multicomponent sol gel silica glasses with a low hydroxyl concentration and uniform distribution of rare earth ions.

A study of the hydroxyl concentration was performed for several Er^{3+} doped sol gel samples. Figure 2 shows the hydroxyl concentration that varied

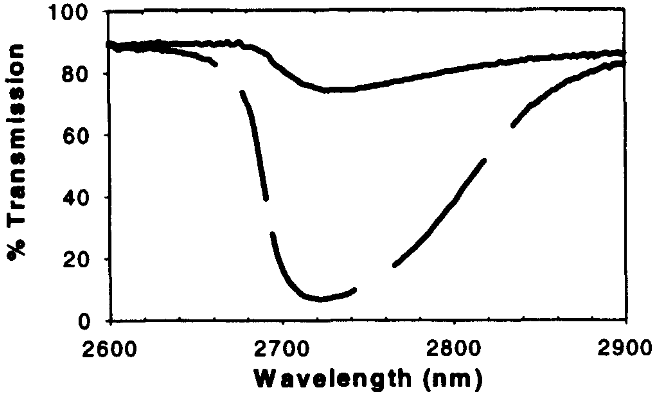

Figure 2 Determination of the hydroxyl concentration in Er doped glasses. The solid line is the multicomponent Er doped sol gel glass. The dashed line is the typical Er doped sol-gel glass.

from 1200 ppm to 56 ppm for the typical Er doped sol gel and the Er multicomponent sol gel respectively.

Er-doped glass prepared through the typical sol-gel process has IR fluorescence with a peak at 1534 nm. However, in the Er multicomponent glasses the peak is at 1540 nm and has an enhanced linewidth and intensity. The peak emission is about 100 times more intense than that from the typical Er doped sol gel glass.

This glass is expected to achieve a gain of 5.4 dB/cm, which is better than the reported values of 4 and 1 dB/cm for phosphate and sol gel waveguides respectively. Thus, the multicomponent glass has a clear edge over the untreated glass in reducing both the hydroxyl concentration and rare earth clustering. This ability has reduced the concentration and hydroxyl quenching observed in Er-doped sol-gel glasses. These glasses are optically transparent and light pink in color. Further studies will focus on lasing action at 1.55 μm and the upconversion properties are underway.

III. Photonic Crystals.

Photon localization, in three-dimensional dielectric photonic crystals, opens a new frontier with its focus on the experimental realization of strong localization of light and its consequences in laser physics[35,36]. In recent years, photonic band-gap (PBG) structures have been shown to lead to the localization of light through the carefully engineered interplay between microscopic scattering resonances and the coherent interference of light from many such scatterers. The basic structure of a photonic crystal consists of a three dimensional periodic arrangement of two dielectrics as shown in figure 3. The refractive index varies at length scales on the order of optical wavelengths. The propagation of light in these materials is analogous to the

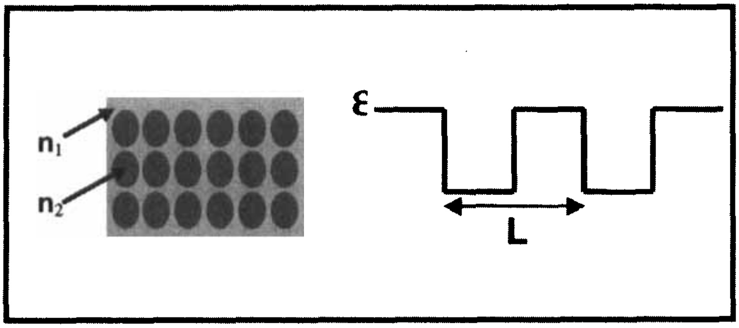

Figure 3 Basic structure for a photonic crystal.

well-known propagation of electrons in a crystalline structure. A photonic band gap material is a special class of photonic crystal in which light is strongly coupled to the crystal. Due to the periodic structure this generates Bragg diffraction and creates a frequency band of light that can not propagate through the crystal in any direction. Since the initial proposal of photonic band gaps, by Professor Sajeev John and Professor Yablonovich, PBG materials exhibiting photon localization have been fabricated at microwave frequencies and more recently, large scale two-dimensional PBG systems have been produced in the near infrared. The ultimate goal for laser applications is a full three-dimensional PBG at optical frequencies in the visible region.

A PBG material is loss-less and comprises a range of frequencies (wavelengths) for which no propagating electromagnetic modes are allowed. Therefore, atoms with transition frequencies within the gap do not experience the usual fluctuations in the electromagnetic vacuum that are responsible for spontaneous decay. Instead, a photon-atom bound state is formed. Unlike the suppression of spontaneous emission in a high-Q optical microcavity, the bound photon may tunnel many optical wavelengths away from the atom before being reabsorbed. The photon density of states is rapidly varying near a photonic band edge, making it dramatically different from the ω^2 dependence found in free space. This implies that the nature of vacuum fluctuations and thus spontaneous emission near a band edge is radically different from the exponential decay found in free space.

Although photonic band gaps are analogous to electronic band gaps in semiconductors, there are many intriguing aspects of photons that are not shared by electronic systems. Among these are laser action and superradiance. These are related to the bosonic nature of light through which many photons can occupy the same mode. The recent observation of laser action in strongly scattering media motivates studies in this new direction[37].

The growth of the photonic crystal was done through the slow sedimentation of monodisperse silica spheres at room temperature. Figures 4a and 4b show the SEM images of crystalline assemblies of 0.48 μm and 0.22 μm silica spheres respectively. These images reveal the FCC packing at the surface and edges of the photonic crystals. Confocal microscopy of the samples also confirmed FCC packing within the photonic crystals.

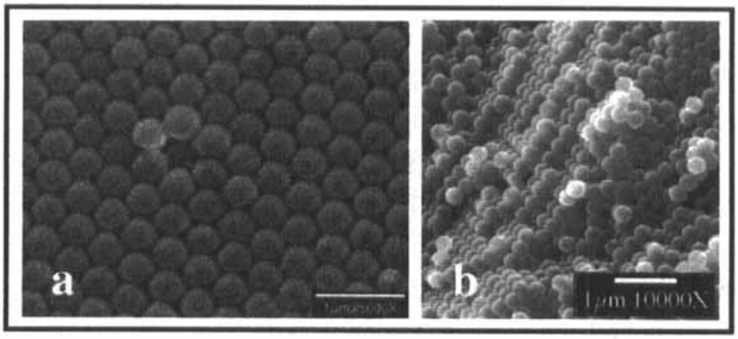

Figure 4 SEM images of crystalline assemblies of SiO_2 spheres. (a) ~480 nm spheres. (b) ~220 nm spheres.

Optical transmission of the crystalline assemblies of 0.48 μm and 0.22 μm silica spheres in chloroform shows the presence of a photonic pseudogap (figures 5a and 5b respectively). By varying the size of the

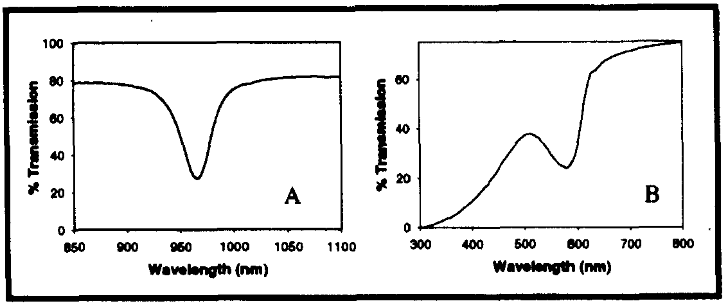

Figure 5 Optical transmission of SiO_2 photonic crystals in chloroform. (A) ~480 nm spheres. (B) ~220 nm spheres.

spheres it is possible to tune the gap across the entire electromagnetic spectrum.

Inverted photonic crystals were prepared from TiO_2 and polystyrene (figures 6a and 6b respectively). The inverted TiO_2 crystals were prepared similar to Wijnhoven and Vos[38] by using polystyrene spheres and a titania precursor followed by the removal of the polystyrene spheres with heating. The inverted polystyrene was prepared through the infiltration of the silica spheres followed by the dissolution of the silica in HF acid.

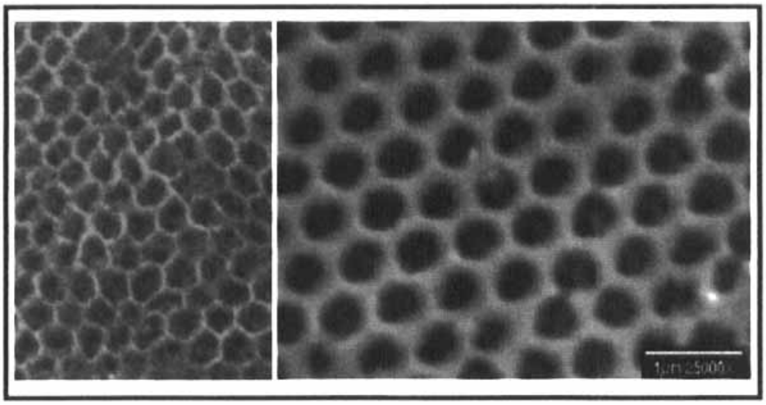

Figure 6 SEM images of inverted photonic crystals. (A) The left image is inverted TiO_2. (B) The right image is inverted polystyrene.

Acknowledgments

This work was supported in part by the Air Force office of Scientific Research MURI program through the University of Southern California, primary contract number 000507 and in part by the Directorate of Chemistry and Life Sciences of the Air Force office of Scientific Research through contract number F49620961O124.

References

[1] R. Burzynski and P. N. Prasad, *Photonics and Nonlinear Optics with Sol-Gel Processed Inorganic Glass: Organic Polymer Composite,*edited by L. C. Klein, (Kluwer Academic, Boston, 1994), Chapter 19.

[2] P. N. Prasad, F. V. Bright, U. Narang, R. Wang, R. A. Dunbar, J. D. Jordan and R. Gvishi, *Hybrid Organic-Inorganic Composites,* Ed. By J. E. Mark, C. Y. -C Lee and P. A. Bianoni, (ACS Symposum series 585, Washington, 1995), Chapter 25.

[3] Y. Wang, A. Suna and J. Mchugh, *J. Chem. Phys., 92,* 6927 (1990).

[4] A. P. Alivisatos, A. L. Harris, N. J. Levinos, M. L. Steigerwald and L. E. Brus, *J. Chem. Phys.,* **89,** 4000 (1988).

[5] A. P. Alivisitos, *Science,* **271,** 933 (1996).

[6] R.K. Jain and R.C. Lind, *J. Opt. Soc. Am.,* **73,** 647 (1983).

[7] N.F. Borelli, D.W. Hall, H.J. Holland and D.W. Smith, *J. Appl. Phys.,* **61,** 5399 (1987).

[8] M. Bruchez, M. Moronne, P. Gin, S. Weiss and A. P. Alivisatos, *Science,* **281,** 2013 (1998).

[9] S. Miltenyi, W. Muller, W. Weichel and A. Radbruch, *Cytometry,* **11,** 231 (1990).

[10] A. P. Alivisatos, K. P. Johnsson, X. G. Peng, T. E. Wilson, C. J. Loweth, M. P. Bruchez, P. G. Schultz, *Nature,* **382,** 609 (1996).

[11] R. Reisfield, E. Yariv and H. Minti, *Opt. Mater.,* **8,** 31 (1997).

[12] (a) H. A. Clark, S. L. R. Barker, M. Brasuel, M.T. Miller, E. Monson, S. Parus, Z. Y. Shi, A. Song, B. Thorsrud, R. Kopelman, A. Ade, W. Meixner, B. Athey, M. Hoyer, D. Hill, R. Lightle and M. A. Philbert, *Sens. Act. B-Chem.,* **51,** 12 (1998) (b) O. V. Makarova, A. E. Ostafin, H. Miyoshi, J. R. Norris and D. Meisel, *J. Phys. Chem.B.,* **103,** 9080 (1999).

[13] H. E. Pudavar, M. P. Joshi, P. N. Prasad and B. A. Reinhardt, *Appl. Phys. Lett.,* **74,** 1338 (1999).

[14] A. S. Dvornikov and P. M. Rentzepis, *Opt. Com.,* **119,** 341 (1995).

[15] M. P. Joshi, H. E. Pudavar, J. Swiatkiewicz, P. N. Prasad and B. A. Reinhardt, *Appl. Phys. Lett.,* **74,** 170 (1999).

[16] X. P. Wang, L. J. Krebs, M. Al-Nuri, H. E. Pudavar, S. Ghosal, C. Liebow, A. A. Nagy, A. V. Schally and P. N. Prasad *Proc. Nat. Acad. Sci.,* **96,** 11081 (1999).

[17] R. C. Willis, *Biophotonics International,* **6,** 42 (1999).

[18] T. F. Towey, A. N. Khan-Lodhi and B. H.Robinson, *J. Chem. Soc.,* **86,** 3757 (1990).

[19] A. Taleb, C. Petit and M. P. Pileni, *Chem. Mater.,* **9,** 950 (1997).

[20] L. Levy, J. F. Hochepied and M. P. Pileni, *J. Phys. Chem.,* **100,** 18322 (1996).

[21] M. Lal, N. D. Kumar, M.P. Joshi and P. N. Prasad, *Chem. Mater.,* **10,** 1065 (1998).

[22] R. Rosetti, R. Hull, J. M. Gibson and L. E. Brus, *J. Chem. Phys.,* **82,** 552 (1985).

[23] M. A. Lopez-Quintela, J. Rivas, *J. Curr. Opin. Coll. Int. Sci.,* **1,** 806 (1996).

[24] J. Eastoe and B. Warne, *J. Curr. Opin. Coll. Int. Sci.,* **1,** 800 (1996).

[25] L. Qi, L. Ma, H. Cheng and Z. Zhao, *Coll. Surf.,* **108,** 117 (1996).

[26] S. Chang, L. Liu and S. A. Asher, *J. Am. Chem. Soc.,* **116,** 6739 (1993).

[27] V. Swayambunathan, D. Hayes, K. H. Schmidt, Y. X. Liao and D. Miesel, *J. Am. Chem. Soc.,* **112,** 3831 (1990).

[28] T. Li, J. Moon, A. A. Morrone, ?. Mecholsky, D. R. Talham and J. H. Adair, *Langmuir,* **15,** 4328 (1999).

[29] E. J. A. Pope and J. D. Mackenzie, *J. Non-Cryst. Solids,* **106,** 236 (1988).

[30] S. K. Lam, X. L. Zhu and D. Co, *App. Phys. B-Las. Opt.,* **68,** 1151 (1999).

[31] X. Orignac, D. Barbier, X. M. Du, R. M. Almeida, O. McCarthy and E. Yeatman, *Opt. Mat.,* **12,** 1 (1999).

[32] H. Fujiwata and K. Sasaki, *J. Appl. Phys.,* **86,** 2385 (1999).

[33] R. Serna, M. J. de Castro, J. A. Chaos, C. N. Alfonso and I. Vickridge, *Appl. Phys. Lett.,* **75,** 4073 (1999).

[34] Y. G. Choi and J. Heo, *Phys. Chem. Glass,* **39,** 311 (1998).

[35] S. John, *Phys. Rev. Lett.,* **58,** 2486 (1987).

[36] E. Yablonovich, *Phys. Rev. Lett.,* **58,** 2059 (1987).

[37] Y. Yamamoto and R. E. Slusher, *Physics Today,* **46,** 66 (1993).

[38] J. E. G. J. Wijnhoven and L. V. Vos, *Science,* **281,** 802 (1998).